

SCIENTIFIC REPORTS

OPEN

Probing the dielectric, piezoelectric and magnetic behavior of $\text{CoFe}_2\text{O}_4/\text{BNT-BT}_{0.08}$ composite thin film fabricated by sol-gel and spin-coating methods

Marin Cernea¹, Bogdan Stefan Vasile², Vasile Adrian Surdu², Roxana Trusca², Cristina Bartha¹, Floriana Craciun³ & Carmen Galassi⁴

We investigated in this paper a novel bilayer composite obtained by sol-gel and spin coating of the ferroelectric $0.92\text{Na}_{0.5}\text{Bi}_{0.5}\text{TiO}_3-0.08\text{BaTiO}_3$ (abbreviated as $\text{BNT-BT}_{0.08}$) and ferromagnetic CoFe_2O_4 phases, for miniature low-frequency magnetic sensors and piezoelectric sensors. This heterostructure, deposited on Si-Pt substrate ($\text{Si-Pt}/\text{CoFe}_2\text{O}_4/\text{BNT-BT}_{0.08}$), was characterized using selected method such as: X-ray diffraction, dielectric spectroscopy, piezoelectric force microscopy, SQUID magnetometry, atomic force microscopy/magnetic force microscopy, and advanced methods of transmission electron microscopy. $\text{CoFe}_2\text{O}_4/\text{BNT-BT}_{0.08}$ ferromagnetic–piezoelectric thin films show good magnetization, dielectric constant and piezoelectric response. The results of analyses and measurements reveal that this heterostructure can have applications in high-performance magnetoelectric devices at room temperature.

In recent years, the manufacture of composite materials from components with different macroscopic properties was studied extensively^{1–5}. These composites have applications in electronic devices with novel distinct functionalities^{6–8}. Oxide heterostructure thin films with electric and magnetic properties were prepared by various techniques, such as: sol-gel⁹, pulsed laser deposition¹⁰, rf sputtering¹¹, tape-casting method¹², etc. There are several reports on composites with electrical, ferroelectric and ferromagnetic behaviors, for example: ferroelectric–ferromagnetic composites ($\text{BiFeO}_3\text{-CoFe}_2\text{O}_4$ ¹³, nickel ferrite–PZT and manganite–PZT⁸, $\text{CoFe}_2\text{O}_4\text{-BaTiO}_3$ ¹⁴) and ferromagnetic–piezoelectric oxide heterostructures ($\text{La}_{0.7}\text{Sr}_{0.3}\text{MnO}_3\text{-PbZr}_{0.2}\text{Ti}_{0.8}\text{O}_3$ ¹⁵, $\text{CoFe}_2\text{O}_4\text{-PZT}$ ¹⁰). There are few reports on lead free ferroelectric ($\text{Na}_{0.5}\text{Bi}_{0.5}\text{TiO}_3$)–magnetostrictive (CoFe_2O_4) particulate composites^{16–19} but bilayer ferrite–piezoelectric composites of CoFe_2O_4 and $\text{BNT-BT}_{0.08}$ have not been reported so far a heterostructure composed of a piezoelectric and a magnetic one.

In this work we have created a heterostructure thin film composed from piezoelectric and magnetic materials. We have investigated the composite thin film $\text{Si-Pt}/\text{CoFe}_2\text{O}_4/\text{BNT-BT}_{0.08}$ in which $\text{BNT-BT}_{0.08}$ and cobalt ferrite (CoFe_2O_4) films were deposited in two subsequent steps on Si-Pt buffer, by sol-gel and spin-coating techniques. Cobalt ferrite was chosen because is an important component for multiferroic heterostructure thin films or composites due to its high coercivity, moderate magnetization and highest magnetostriction coefficient²⁰. ($\text{Bi}_{0.5}\text{Na}_{0.5}$) TiO_3 (BNT) doped with BaTiO_3 (BT) is selected as ferroelectric layer because $\text{BNT-BT}_{0.08}$ is considered a good candidate to replace the lead-based piezoelectric materials^{21,22}. It has been shown previously that the $(1-x)\text{BNT-xBT}$ (BNT-BT_x) solid solution has in the compositional domain $x = 0.06-0.10$ a nearly morphotropic phase boundary (MPB)^{23,24} where rhombohedral $\text{Bi}_{0.5}\text{Na}_{0.5}\text{TiO}_3$ and tetragonal BaTiO_3 phases coexist. Compared

¹National Institute of Materials Physics, P.O. Box MG-7, Bucharest-Magurele, 077125, Romania. ²University POLITEHNICA of Bucharest, 060042, Bucharest, Romania. ³Istituto di Struttura della Materia-CNR (ISM-CNR), Area di Ricerca di Tor Vergata, I-, 00133, Roma, Italy. ⁴CNR-ISTEC, Institute of Science and Technology for Ceramics, Via Granarolo 64, I-, 48018, Faenza, Italy. Correspondence and requests for materials should be addressed to B.S.V. (email: bogdan.vasile@upb.ro)

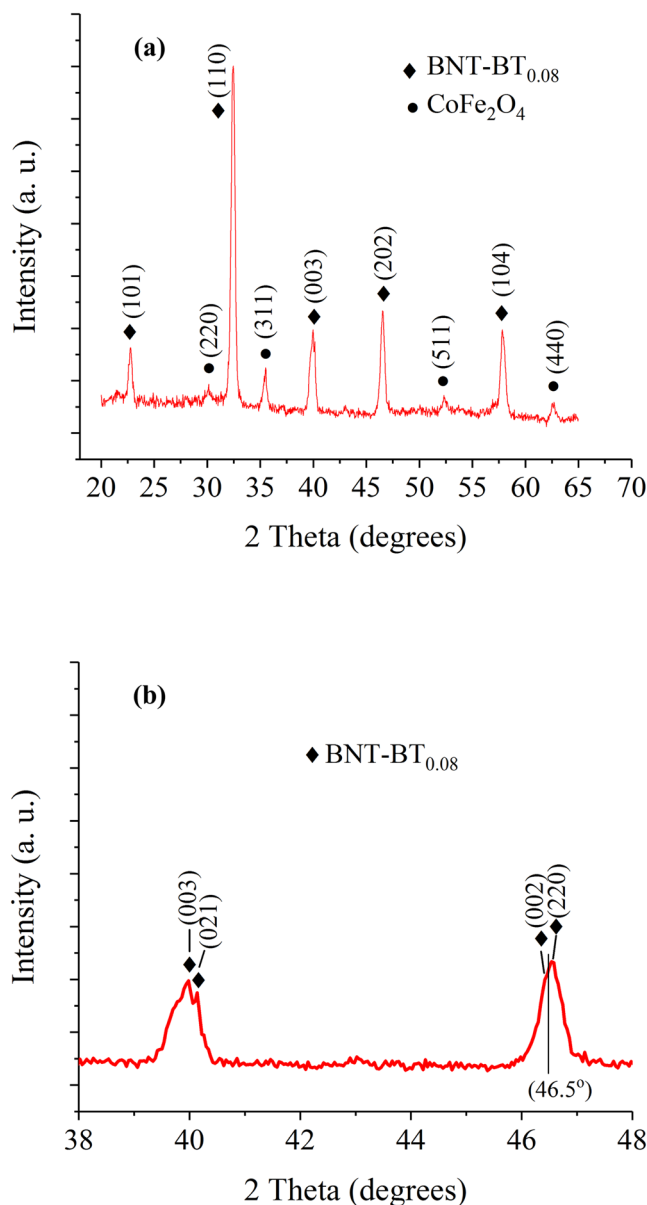


Figure 1. (a) XRD patterns of the Si-Pt/CoFe₂O₄/BNT-BT_{0.08} heterostructure thin film and (b) detail between 38° and 48°.

with BNT ceramic, the BNT-BT_{0.08} composition placed in the MPB provides improved poling and piezoelectric properties^{23,25}.

Results and Discussion

Structural characterization of Si-Pt/CoFe₂O₄/BNT-BT_{0.08} bilayer heterostructure. XRD spectra recorded in grazing incidence diffraction geometry of the Si-Pt/CoFe₂O₄/BNT-BT_{0.08} heterostructure thin film are shown in Fig. 1.

As expected, it can be observed that the sample is biphasic (CoFe₂O₄ and BNT-BT_{0.08}). All the diffraction peaks could be indexed with a spinel structure (Fd3m space group) for CoFe₂O₄ phase (JCPDS: 04-005-7078)²⁶ and a perovskite rhombohedral structure for Bi_{0.5}Na_{0.5}TiO₃ rhombohedral phase (JCPDS: 04-015-0482)²⁷, respectively. The rhombohedral phase of BNT-BT_{0.08} layer at room temperature, is characterized by (003)/(021) peak splitting between 39° and 41° and, a single (202) peak between 45° and 48°, as indicates the JCPDS: 04-015-0482²⁷ while BNT-BT_{0.08} tetragonal phase shows splitting of the (200) and (220) peaks at $2\theta \sim 46.5^\circ$ (JCPDS: 04-011-3919)²⁸. Figure 2(b) shows a not symmetrical peak at 45°, that can be deconvoluted in the (200) and (220) peaks, suggesting the existence of BNT-BT_{0.08} tetragonal phase. This result is in good agreement with the paper of Xu *et al.*²⁹, which reported that the MPB of BNT-BT_x exists for $0.06 < x < 0.10$.

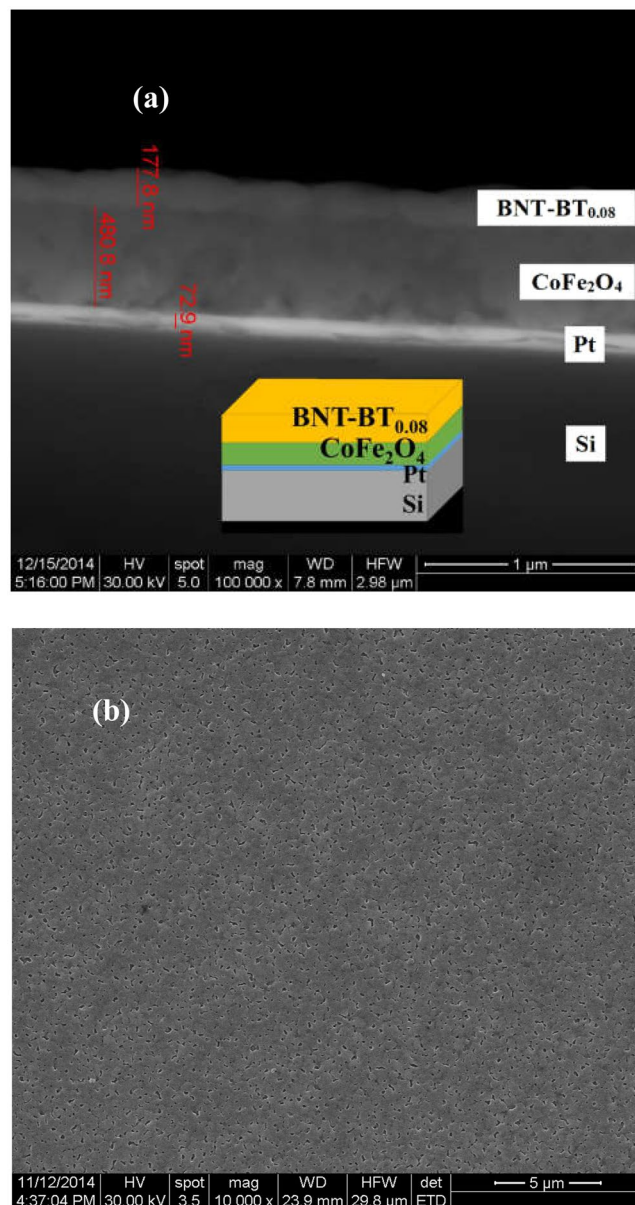


Figure 2. (a) Cross-section SEM image of Si-Pt/CoFe₂O₄/BNT-BT_{0.08} heterostructure thin film and a schematic representation inset; (b) SEM image of the composite film surface.

Figure 2 shows the SEM images obtained by backscattering for Si-Pt/CoFe₂O₄/BNT-BT_{0.08} heterostructure thin film. The surface of BNT-BT_{0.08} top film of Si-Pt/CoFe₂O₄/BNT-BT_{0.08} heterostructure shows pores formed as a result of the removal of the organic species during the calcination of the film gel. (Fig. 2(b)).

The cross-section and plan-view images of the heterostructure thin film indicate a granular structure, specific for the thin films prepared by the sol-gel method, with grain of polyhedral shape and various sizes. As can be seen on Fig. 2(a,b), some pores on the surface are connected while the internal pores are in small quantities and not connected. Therefore, the porosity of the surface is much higher than internal porosity. No intermediate layer is observed and the interface between CoFe₂O₄ and BNT-BT_{0.08} layers is clear, which suggests that both single-phase CoFe₂O₄ and BNT-BT_{0.08} films can coexist without interface diffusion. Thus results are agreement with the XRD patterns.

As it results from BSE/SEM image in Fig. 2(a), the thickness of BNT-BT_{0.08} layer is in the 150–180 nm range, while the thickness of CoFe₂O₄ bottom layer is about 480–490 nm.

Cross-sectional transmission electron microscopy shows BNT-BT_{0.08} top layer with thickness of 116 nm deposited on CoFe₂O₄ thin film of 568 nm thickness (Fig. 3(a)).

The high resolution TEM images (Fig. 3(b,c)) confirm the existence of CoFe₂O₄ cubic phase ($d = 2.53 \text{ \AA}$ and (311) plane) and Na_{0.5}Bi_{0.5}TiO₃ rhombohedral phase ($d = 2.75 \text{ \AA}$ corresponding to the (104) crystallographic plane).

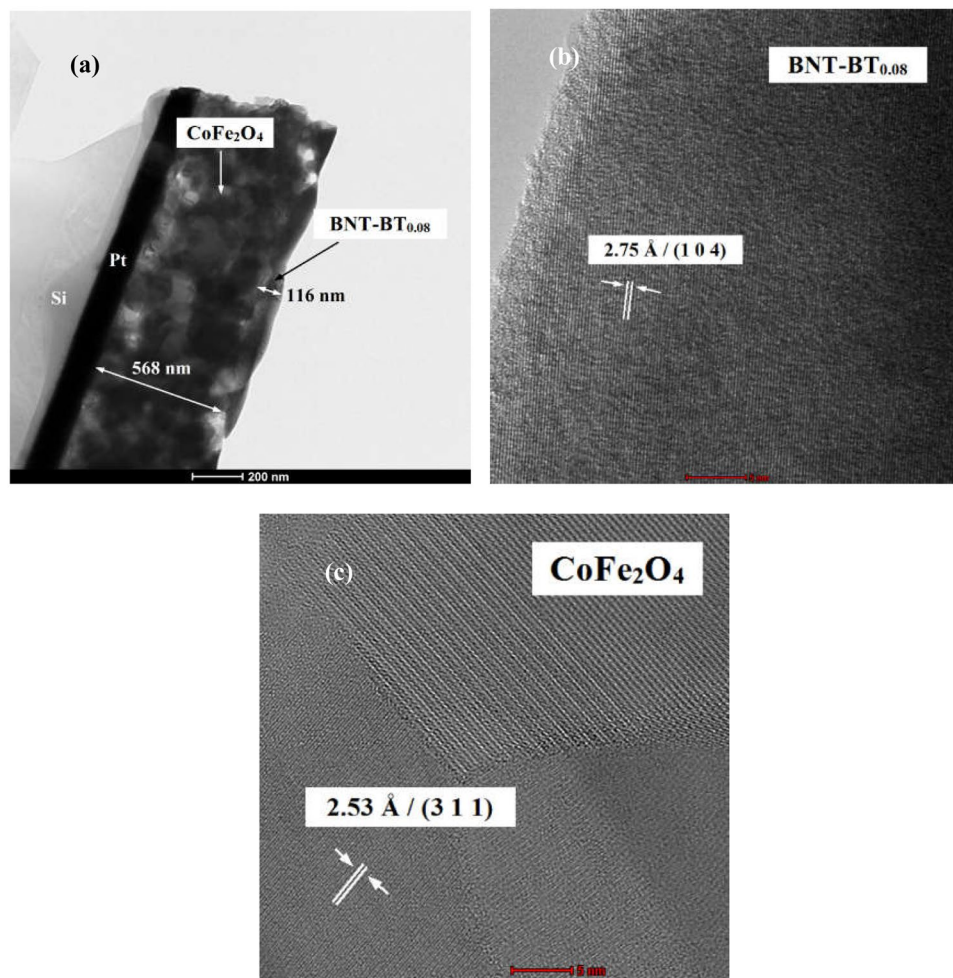


Figure 3. (a) TEM image of Si-Pt/CoFe₂O₄/BNT-BT_{0.08} heterostructure thin film, (b) HR-TEM image of BNT-BT_{0.08} layer and (c) HR-TEM image of CoFe₂O₄ layer.

High-angle annular dark-field (HAADF) imaging in scanning transmission electron microscopy (STEM) was also used in order to further confirm the bilayered structure of Si-Pt/CoFe₂O₄/BNT-BT_{0.08} composite (Fig. 4).

As can be seen in Fig. 4(a), the two chemically different layers (CoFe₂O₄ and BNT-BT_{0.08}) are clearly distinguished from each other. Elemental mapping clearly shows the homogenous dispersion of Co, Fe, Bi, Na and Ti elements into their corresponding layers (Fig. 4(c–g)).

Magnetic properties. The magnetic hysteresis loops of Si-Pt/CoFe₂O₄/BNT-BT_{0.08} bilayer heterostructure (Fig. 5(a,b)) were recorded at 5 K and 295 K, under a magnetic field of ≤ 70 kOe, perpendicular to the BNT-BT_{0.08} layer plane.

The composite CoFe₂O₄/BNT-BT_{0.08} exhibits magnetic hysteresis loops at 5 K and 295 K (Fig. 5(ab)), indicating an ordered magnetic structure. The hysteresis loops show a negative slope with value of $-2 \cdot 10^{-3}$ (emu/cm³)/Oe, due to the diamagnetic signal.

The values of remnant magnetization (M_r), saturation magnetization (M_s), and coercive magnetic field (H_c) of the CoFe₂O₄/BNT-BT_{0.08} thin film heterostructure, after diamagnetic corrections, are listed in Table 1.

As can be seen in Table 1, the magnetic parameters are higher for the CoFe₂O₄/BNT-BT_{0.08} composite thin film because the CoFe₂O₄ layer in this composite is thicker and has the crystallites larger than the CoFe₂O₄ layer in the BNT-BT_{0.08}/CoFe₂O₄ composite structure³⁰. These results are in good agreement with ref.³¹. In the CoFe₂O₄/BNT-BT_{0.08} bilayered heterostructure, the thickness of CoFe₂O₄ bottom layer is about 480–490 nm and crystallites size of ~ 65 nm while in the BNT-BT_{0.08}/CoFe₂O₄ composite thin film, the thickness of CoFe₂O₄ layer is ~ 280 nm and crystallites size is ~ 20 nm³⁰.

The low values of magnetization and coercive field, as well as the diamagnetic component of magnetization, indicate the behavior of a diluted magnetic oxide which may be due to Bi_{0.5}Na_{0.5}TiO₃ and BaTiO₃ (BNT-BT_{0.08}) which are considered as diluted magnetic oxide³² and also, due of a very small contributions of the oxides from substrate. As we mentioned, the substrate is made of Si/SiO₂(450 nm)/TiO₂(15 nm)/Pt(100 nm); TiO₂ being recognized as diluted magnetic oxide³³, like also SiO₂³⁴.

The different component phases of the heterostructures, their crystallographic parameters, the thickness ratio between the magnetic and piezoelectric phases, the stress condition and the nature of the substrate are factors

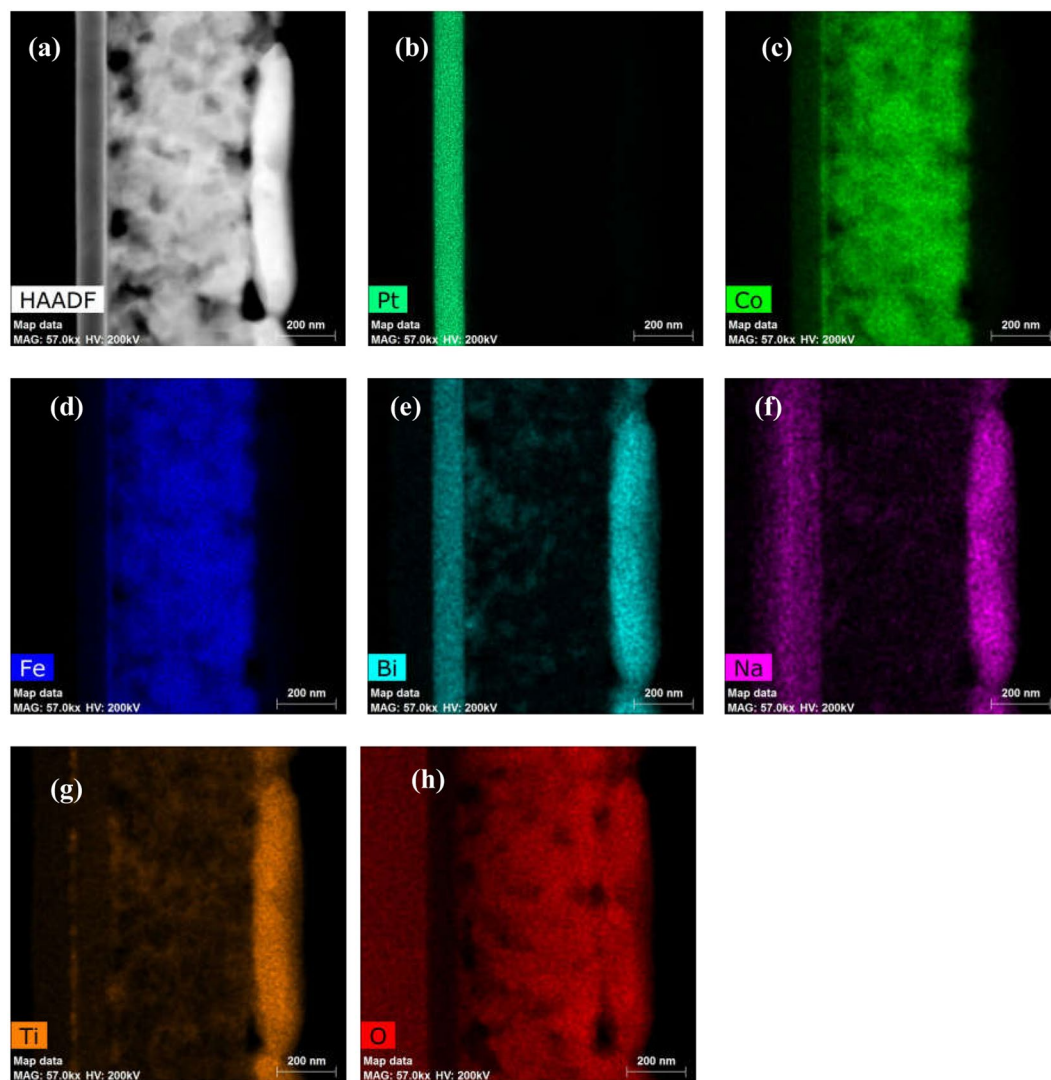


Figure 4. STEM of Si-Pt/CoFe₂O₄/BNT-BT_{0.08} heterostructure thin film. (a) High-angle annular dark-field imaging (HAADF). (c–h) Elemental maps of Co (c), Fe (d), Bi (e), Na (f), Ti (g) and O (h) for CoFe₂O₄/BNT-BT_{0.08} bilayered composite deposited on Pt (b) substrate.

that reduce the magnetic parameters of our heterostructure compared with ferromagnetic–piezoelectric bilayer composites previously reported^{10,33}. CoFe₂O₄ is a hard magnetic material with high coercivity and moderate magnetization. BNT-BT_{0.08} layer deposited on CoFe₂O₄ influences the magnetization of the heterostructure by the residual strain which appears at the CoFe₂O₄/BNT-BT_{0.08} interface, as has been reported for CoFe₂O₄-PZT bilayers^{10,35}.

The bright and dark contrast of ferromagnetic domains indicates opposite direction of the magnetization, perpendicular to the surface of thin film. As can be seen in Fig. 6, Si-Pt/CoFe₂O₄/BNT-BT_{0.08} bilayered heterostructure shows magnetic domain at grains boundary and aggregates boundary region. The MFM images reveal magnetic properties for the composite film Si-Pt/CoFe₂O₄/BNT-BT_{0.08} and, a nanoscale magnetic domain configuration.

Dielectric spectroscopy, tunability and leakage current measurements. Figure 7 shows results of the dielectric spectroscopy measurements obtained for the bilayered heterostructure CoFe₂O₄/BNT-BT_{0.08} (Fig. 7(a,b)). The two different curves correspond to different capacitors (A and B). As can be seen in Fig. 7(a), the dielectric constant increases at low frequency and remains constant at higher frequency.

One must take into account the heterostructure type of the samples, with a layer of CoFe₂O₄ deposited over the ferroelectric layer BNT-BT_{0.08}. The dielectric measurements are performed on the capacitor between the bottom electrode (Pt) and the top electrode (Au foil) applied over the CoFe₂O₄ layer. Therefore the measurements are carried out over a very small capacitance (CoFe₂O₄) in series with a high capacitance (BNT-BT_{0.08}) which results in an equivalent capacitance smaller than that of CoFe₂O₄ layer. This explains the small dielectric constant of the heterostructure.

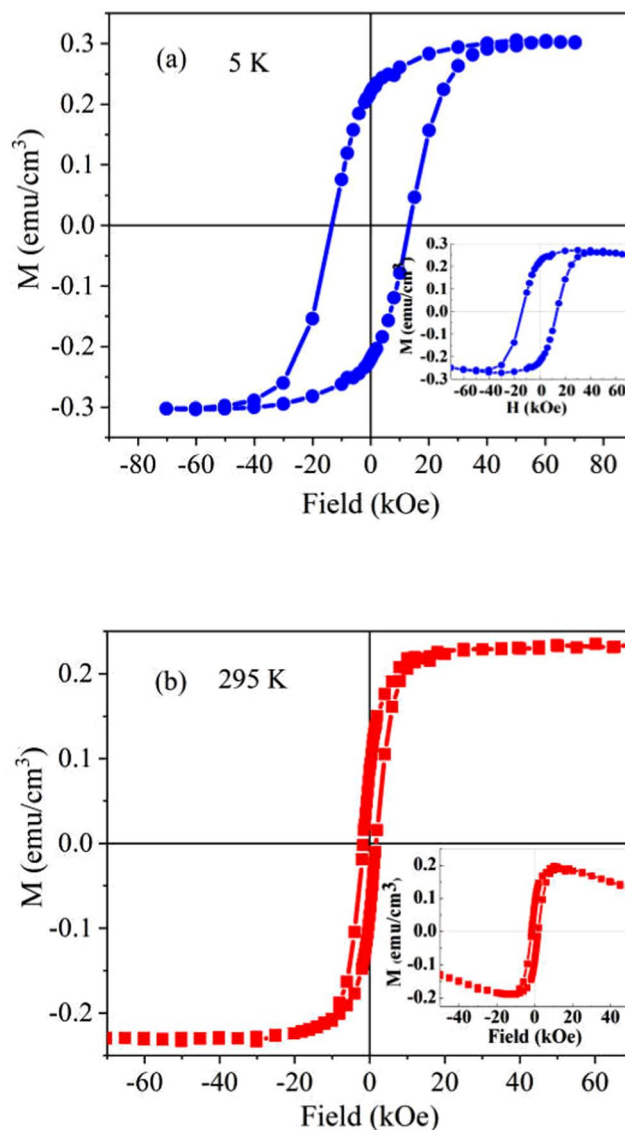


Figure 5. Magnetic hysteresis curves recorded at (a) 5 K and (b) 295 K for Si-Pt/CoFe₂O₄/BNT-BT_{0.08} layered composite.

Heterostructure films samples	Temp. (K)	M_s (emu/cm ³)	M_r (emu/cm ³)	H_c (kOe)
Si-Pt/CoFe ₂ O ₄ /BNT-BT _{0.08}	5	0.3	0.22	13.63
	295	0.23	0.086	1.7
Pb(Zr _{0.52} Ti _{0.48})O ₃ /CoFe ₂ O ₄ /SrTiO ₃ ¹⁰	RT	35.8	14.85	0.1
BNTKNNLTS-CZFM ⁴⁴	RT	13.85	~0.50	7.5 × 10 ⁻³
Si-Pt/BNT-BT _{0.08} /CoFe ₂ O ₄ ³⁰	5	0.136	0.08	15
	295	0.1	0.012	0.27

Table 1. Magnetic parameters of the CoFe₂O₄/BNT-BT_{0.08} bilayered heterostructure measured at 5 K and 295 K (results from the literature are reported as well, for comparison). In Table 1: RT is the room temperature, SrTiO₃ (100) single crystal is the substrate, BNTKNNLTS is (Bi_{0.5}Na_{0.5}TiO₃)_{0.97}(K_{0.47}Na_{0.47}Li_{0.06}Nb_{0.74}Sb_{0.06}Ta_{0.2}O₃)_{0.03} and CZFMO is Co_{0.6}Zn_{0.4}Fe_{1.7}Mn_{0.3}O₄.

CoFe₂O₄/BNT-BT_{0.08} structure shows high dielectric constant and high ac conductivity at low frequency (below 1 kHz) which indicates a strong contribution of relaxation processes associated with conductivity (due to oxygen vacancies and other defects) in this sample. Variation of the dielectric properties with frequency of the heterostructure thin film can be due to an extrinsic behavior resulting from the microstructure deficiency.

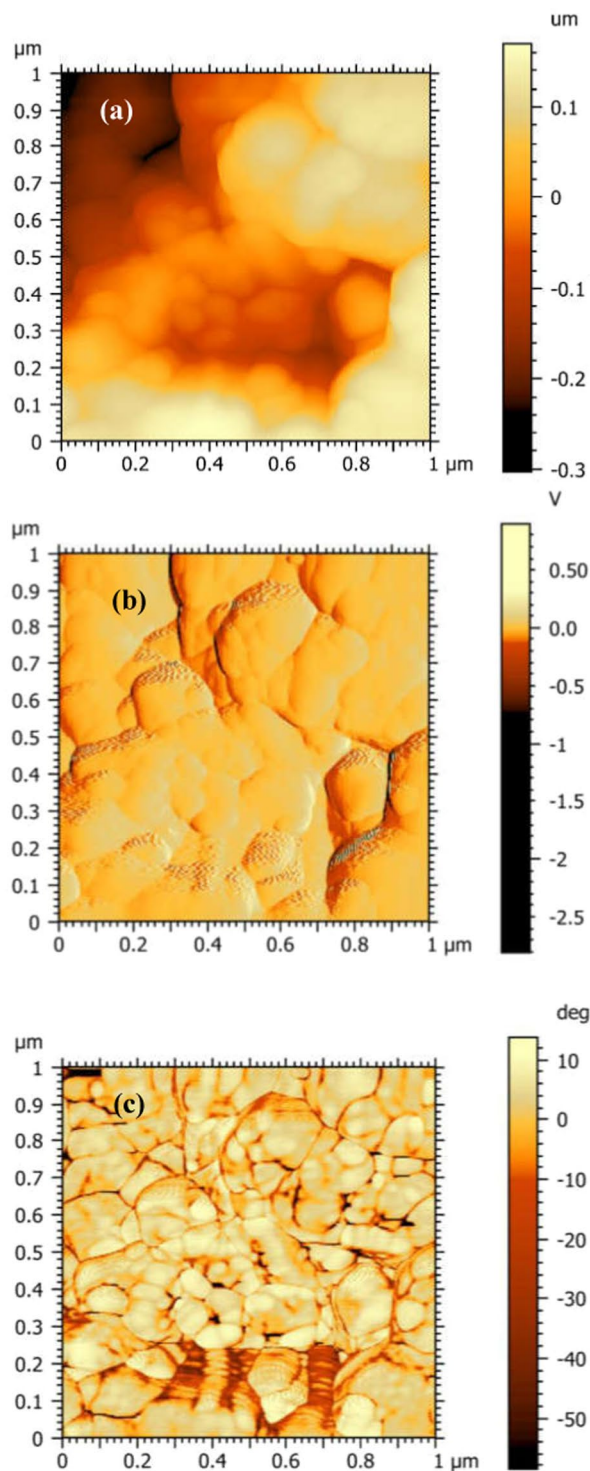


Figure 6. (a) AFM image and (b,c) MFM images: (b) amplitude and (c) phase for Si-Pt/CoFe₂O₄/BNT-BT_{0.08} layered heterostructure.

The deviation from flat conductivity at low-frequency is also due to the interface between the layers and the electrodes.

In ref.⁸, it has been reported that with increasing CoFe₂O₄ film thickness, the frequency dependence of dielectric constant becomes gradually stronger, due to Maxwell-Wagner polarization mechanism^{36,37}. In multiphase composites, Maxwell-Wagner polarization at the interface of ferroelectric-ferromagnetic phases would lead to strong dependence of dielectric constant especially at low frequency³⁸.

Measurements of the dielectric permittivity of samples under a dc bias electric field E yield the tunability factor (n_r), according to the formula:

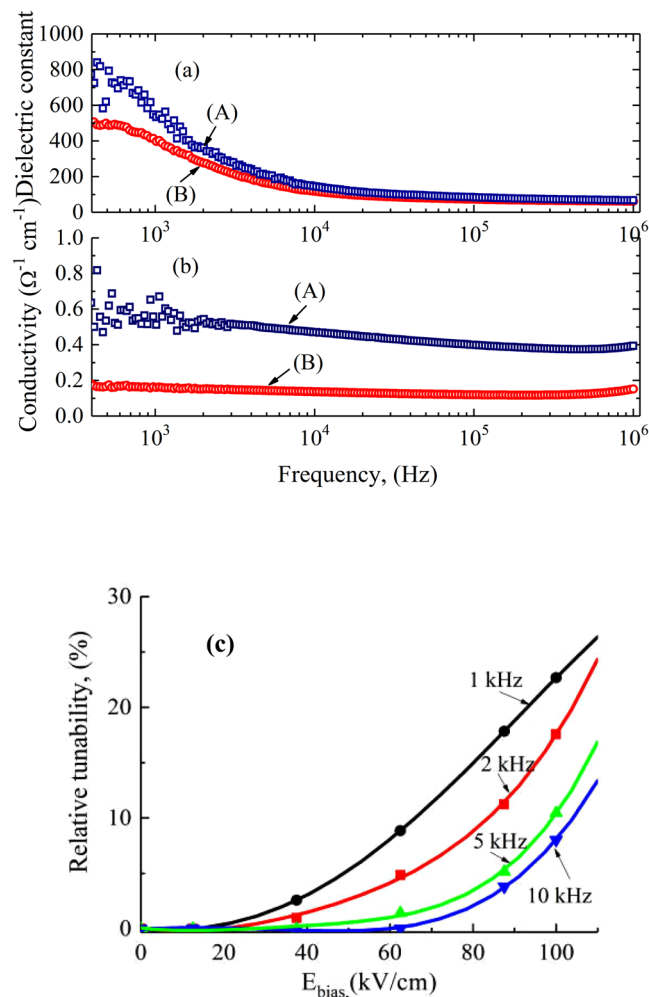


Figure 7. (a) Dielectric constant, (b) ac conductivity and (c) relative tunability for the Si-Pt/CoFe₂O₄/BNT-BT_{0.08} heterostructure thin films.

$$n_r = \frac{\varepsilon(0) - \varepsilon(E)}{\varepsilon(0)} \quad (1)$$

where $\varepsilon(E)$ is the dielectric constant under bias and $\varepsilon(0)$ is the dielectric constant without bias electric field. The results for the CoFe₂O₄/BNT-BT_{0.08} sample are shown in Fig. 7(c). It can be observed that the CoFe₂O₄/BNT-BT_{0.08} heterostructure displays a tunability of 23% at 1 kHz and 100 kV/cm. This value decreases strongly when the frequency increases. This decreasing is associated with the strong dependence of dielectric constant on frequency.

Leakage current density is a key factor for multiphase composite thick film and reflects the quality and reliability of a film. Therefore, it is important to investigate the leakage property and conduction mechanisms of the films. Leakage current measurements for the CoFe₂O₄/BNT-BT_{0.08} bilayer composite have been made at ambient temperature. The results are shown in Fig. 8(a,b).

It can be observed from Fig. 8(a) that the leakage current density shows symmetrical positive and negative arms. Leakage current density has the lowest value of about $1.5 \cdot 10^{-4}$ A/cm² at low electric field and shows a strong increase with electric field. The highest value of the current density measured on Si-Pt/CoFe₂O₄/BNT-BT_{0.08} heterostructure thin film, at an electric field of 200 kV/cm, was $4.0 \cdot 10^{-1}$ A/cm² (Fig. 8(a)). The leakage current is mainly attributed to conduction through grain boundaries in the BNT-BT_{0.08} layer³⁹.

The parameters of the $J(E)$ dependence law can give information about the possible conduction mechanisms in the composite structure. Thus a dependence of the type:

$$J \propto E^2 \quad (2)$$

is characteristic for a space charge-limited conduction (SCLC) mechanism^{40,41}. Alternatively, a dependence of the type:

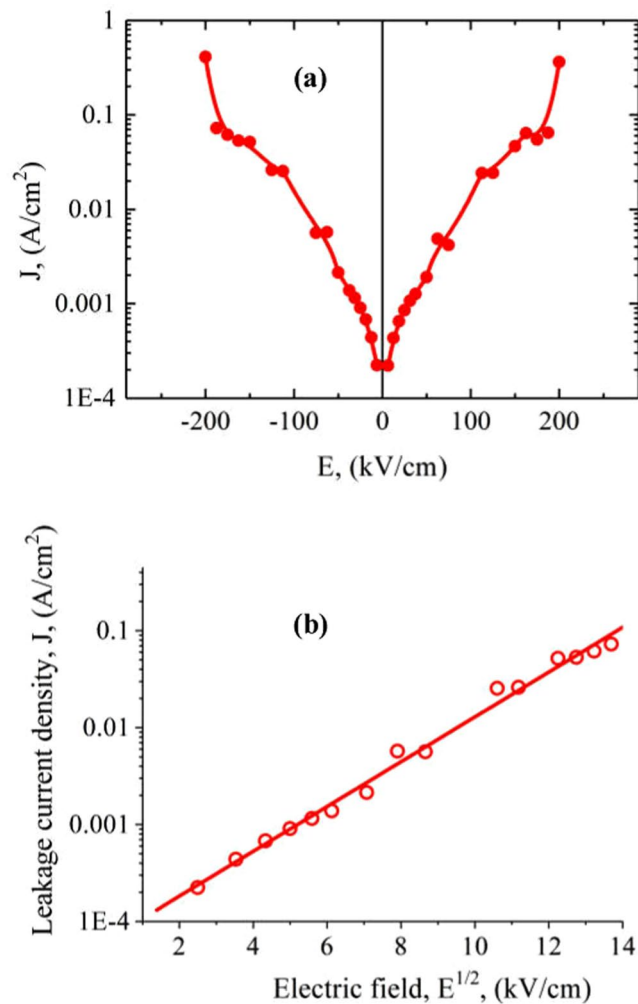


Figure 8. (a) Leakage current density (J) dependence on electric field E for the Si-Pt/CoFe₂O₄/BNT-BT_{0.08} heterostructure thin films; (b) leakage current density represented as a function of the square root ($E^{1/2}$) of the field.

$$J \propto e^{-\frac{1}{kT}(\Phi - aE^{1/2})} \quad (3)$$

is characteristic for a Schottky-type conduction mechanism^{40,42}, related to the potential barrier created by the different Fermi levels of dielectric and metal. In equation (3), Φ is the height of the Schottky barrier height, a is a material constant and k is the Boltzmann constant^{40,41}. Thus by plotting the obtained data as a function of E^2 or $E^{1/2}$ (on a semilogarithmic scale) it is helpful to discern among the different possible conduction mechanisms. For the CoFe₂O₄/BNT-BT_{0.08} heterostructure the plot of J vs E^2 (not shown here) clearly showed that this law is not obeyed for any electric field range, therefore a SCLC mechanism was ruled out. Instead, as can be observed from Fig. 8(b), a plot of J (in log scale) vs $E^{1/2}$ clearly shows that the leakage current is controlled by a Schottky barrier-type mechanism in almost all the field range.

It is concluded that the leakage mechanism found for the investigated heterostructure points to the dominant role of the interfaces between the CoFe₂O₄ and BNT-BT_{0.08} and between these layers and the hybrid electrodes in the leakage current measurements.

Piezoelectric properties. The ferroelectric behavior of the bilayered heterostructure CoFe₂O₄/BNT-BT_{0.08} was investigated by piezoelectric force microscopy (PFM) and their out-of-plane piezoelectric response is presented in Figs 9 and 10.

In the piezoelectric images, domains with opposite polarities exhibit different phase contrast. The CoFe₂O₄/BNT-BT_{0.08} composite thin film exhibits good piezoresponse over a large area (Fig. 9(b,c)). From the cross-section analysis, which simultaneously investigates the surface morphology (grain size) (Fig. 9(d)) and domain populations (domain size and response signal) (Fig. 9(e)), it can be seen that a majority of the domains, randomly distributed in the composite, have dimensions smaller than the grain size, suggesting a ferroelectric multidomains structure for the grains. Figure 10(a,b) reveal typical remnant piezoresponse amplitude and phase measurements, respectively, recorded as a function of applied dc voltage.

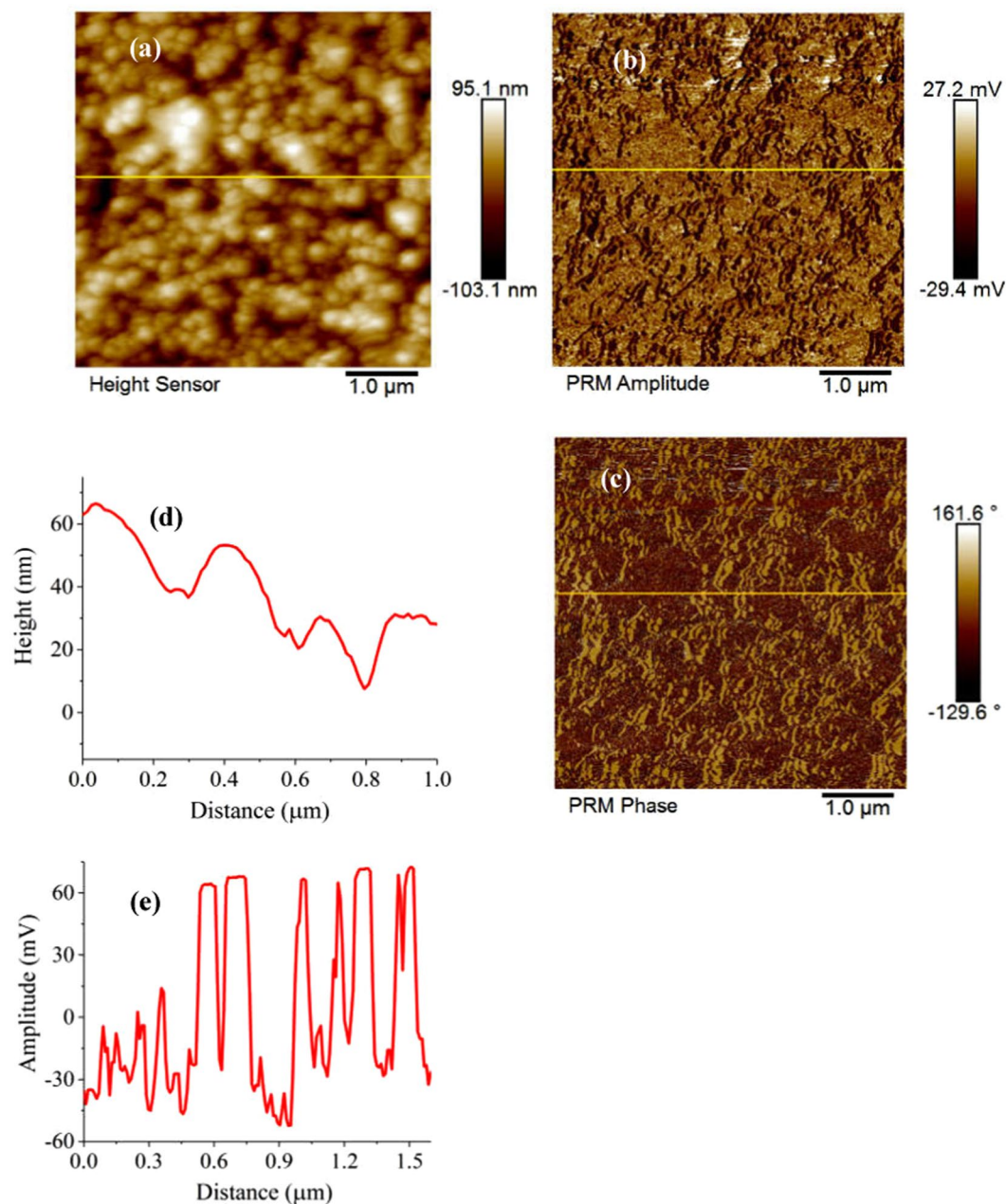


Figure 9. (a) AFM image, (b,c) PFM images: (b) amplitude and (c) phase, (d) line profile analysis of the morphology and (e) of the piezoresponse signal amplitude for the Si-Pt/CoFe₂O₄/BNT-BT_{0.08} heterostructure thin film.

The polarization switching and hysteresis show clearly that the Si-Pt/CoFe₂O₄/BNT-BT_{0.08} bilayer thin film is ferroelectric at nanoscale level.

In summary, bilayer composite CoFe₂O₄/BNT-BT_{0.08} was deposited on Si-Pt substrate by spin-coating technique. This heterostructure thin film presented CoFe₂O₄ cubic phase and BNT-BT_{0.08} phase crystallized on the lattices of rhombohedral and tetragonal Bi_{0.5}Na_{0.5}TiO₃. The composite CoFe₂O₄/BNT-BT_{0.08} film shows ferromagnetic, ferroelectric and piezoelectric properties. The values of magnetic parameters for CoFe₂O₄/BNT-BT_{0.08} heterostructure, with nanoscaled magnetic domain, were: $M_s = 0.23 \text{ emu/cm}^3$, $M_r = 0.086 \text{ emu/cm}^3$ and $H_c = 1.7 \text{ kOe}$, at 295 K. CoFe₂O₄/BNT-BT_{0.08} structure shows high dielectric constant $\epsilon_r = 548$ at 1 kHz and room temperature and good tunability of 23% at 1 kHz. PFM investigations suggested a ferroelectric multidomains structure for the grains of this composite thin film. The ratio of magnetic and electric properties of this composite depends on the thickness ratio of magnetic and piezoelectric layers. These results demonstrate the possibility of manufacturing 2-D materials for sensors with multiple functionalities (ferromagnetic, ferroelectric and piezoelectric).

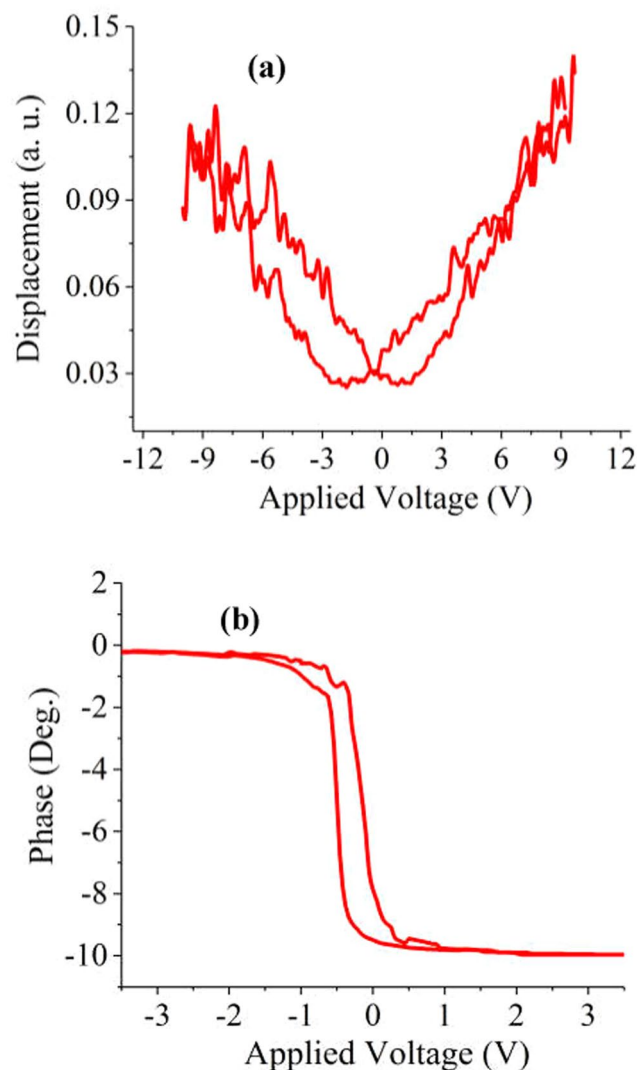


Figure 10. Local PFM hysteresis loops: (a) amplitude signal and (b) phase signal of Si-Pt/CoFe₂O₄/BNT-BT_{0.08} heterostructure thin film.

Methods

Si-Pt/CoFe₂O₄/BNT-BT_{0.08} ferromagnetic–piezoelectric bilayer composite was prepared on Si-Pt substrates, as follows. In the first step, 10 layers of CoFe₂O₄ were deposited on Si-Pt by spin-coating technique. The as-obtained thin film was calcined at 700 °C for 1 h, in air, in order to crystallize CoFe₂O₄. In the second step, 10 layers of BNT-BT_{0.08} sol-precursor were deposited by spin-coating on the cobalt ferrite thin film prepared earlier. The new structure was calcined at 800 °C for 5 min, in oxygen to crystallize the layer of BNT-BT_{0.08}. The precursor sols of CoFe₂O₄ and BNT-BT_{0.08} were prepared by sol-gel technique as described in our previous works^{42,43}, respectively. According to these reports, CoFe₂O₄ precursor sol was prepared from cobalt acetate (Co(CH₃CO₂)₂·4H₂O, 99.995%, Sigma-Aldrich), iron nitrate (Fe(NO₃)₃·9H₂O, 99.99%, Sigma-Aldrich), citric acid (C₆H₈O₇, 99%, Sigma-Aldrich), ethanol, acetic acid and distilled water. The precursor sol of BNT-BT_{0.08} was prepared from bismuth (III) acetate ((CH₃COO)₃Bi, 99.99%, Sigma-Aldrich), sodium acetate (CH₃COONa, 99.995%, Sigma-Aldrich), barium acetate ((CH₃COO)₂Ba, 99%, Sigma-Aldrich), titanium (IV) isopropoxide (Ti{OCH(CH₃)₂}₄) in isopropanol (Sigma-Aldrich), acetic acid, acetylacetone and formamide. In order to prepare CoFe₂O₄ precursor sol, the iron nitrate was dissolved in ethanol and separately, the amount of citric acid was dissolved in ethanol, at room temperature. The cobalt acetate was dissolved in a mixture of ethanol, acetic acid and water, at room temperature. The citric acid solution was added to the mixture solutions of Fe and Co, in a molar ratio of Co:Fe: citric of 1:2:3, and a cobalt ferrite precursor sol was obtained. The as obtained sol was used for deposition of CoFe₂O₄ thin film on Si-Pt substrate.

BNT-BT_{0.08} precursor gel was prepared using the following strategy: first, was prepared a mixture of sodium, bismuth and barium acetic solutions and separately, a mixed solution of titanium isopropoxide: isopropanol: acetylacetone in the volume ration 1:2:0.5. The complex solution of Na, Bi and Ba was added to the titanium isopropoxide solution under continuous magnetic stirring and heating at 85 °C, and a sol precursor of BNT-BT_{0.08}

was prepared. Acetylacetone is used as stabilizer for the sol while formamide (N, N-dimethylformamide, Aldrich) was used in order to avoid formation of the cracks in BNT-BT_{0.08} gel film during the thermal treatments of drying and crystallization. The films of CoFe₂O₄ and BNT-BT_{0.08} were deposited by spin casting at 3000 rpm for 20 seconds. After spin coating, the thin films were heated at 200 °C for 2 min to evaporate the solvent, and then at 400 °C for 4 min in air to eliminate organic components. The films were prepared by repeating (10 times) the deposition and pyrolysis cycle. The coated films of CoFe₂O₄ and BNT-BT_{0.08} were annealed at 700 °C for 1 h, in air, in order to crystallize CoFe₂O₄ and at 800 °C for 5 min, in oxygen to crystallize the layer of BNT-BT_{0.08}. Thus, the final product is a Si-Pt/CoFe₂O₄/BNT-BT_{0.08} heterostructure thin film.

The structure of the heterostructure thin film was investigated by using a Bruker-AXS tip D8 ADVANCE diffractometer while the microstructure was investigated with a FEI QUANTA INSPECT F scanning electron microscope (SEM) with field emission gun and a TecnaiTM G² F30 S-TWIN transmission electron microscope (TEM) with a line-resolution of 1 Å, in high resolution transmission electron microscopy (HRTEM) mode. The crystalline structure of the samples was investigated also the selected area electron diffraction (SAED) method. A Titan Themis 200, transmission and scanning transmission electron microscope (S/TEM) was used for analysis of the chemical elements present in the samples. The magnetic hysteresis loops of the bilayer composite were recorded using a Quantum Design MPMS-5S SQUID magnetometer, in the temperature range of 5–355 K and an applied magnetic field of ≤3580 kA/m. The out-of-plane magnetic characteristics of the samples were observed with an atomic force microscope/magnetic force microscope (AFM/MFM), Model 5400, from Agilent Technology. Measurements of the capacitance and dielectric loss have been carried out with an HP 4194A impedance bridge under an electric bias field with variable amplitude. A Radiant Technologies RT-66A system has been employed for measurements of leakage currents on the same heterostructure samples. PFM measurement of local piezoresponse was performed using a sequence of DC switching bias from −3 V to +3 V, superimposed on a AC modulation bias with a frequency of 14 kHz, using a PFM tip directly on the heterostructure surface.

References

- Ma, J., Hu, J. M., Li, L. & Nan, C. W. Recent progress in multiferroic magnetoelectric composites: from bulk to thin films. *Adv. Mater.* **23**, 1062–1087 (2011).
- Lahtinen, T. H. E., Franke, K. J. A. & Van Dijken, S. Electric-field control of magnetic domain wall motion and local magnetization reversal. *Sci. Rep.* **2**, 258 (2012).
- Shimakawa, Y., Azuma, M. & Ichikawa, N. Multiferroic Compounds with Double-Perovskite Structures. *Materials* **4**, 153–168 (2011).
- Dean, J., Bryan, M. T., Schrefl, T. & Allwood, D. A. Stress-based control of magnetic nanowire domain walls in artificial multiferroic systems. *J. Appl. Phys.* **109**, 023915–023915-5 (2011).
- Xie, S., Ma, F., Liu, Y. & Li, J. Multiferroic CoFe₂O₄-Pb(Zr_{0.52}Ti_{0.48})O₃ core-shell nanofibers and their magnetoelectric coupling. *Nanoscale* **3**, 3152–3158 (2011).
- Lahtinen, T. H. E., Tuomi, J. O. & van Dijken, S. Pattern transfer and electric-field-induced magnetic domain formation in multiferroic heterostructures. *Adv. Mater.* **23**, 3187–3191 (2011).
- Trassin, M. Low energy consumption spintronics using multiferroic heterostructures. *J. Phys. Condens. Matter.* **28**, 033001 (2016).
- Hu, Z. *et al.* Non-volatile ferroelectric switching of ferromagnetic resonance in NiFe/PLZT multiferroic thin film heterostructures. *Sci. Rep.* **6**, 32408 (2016).
- Babu, S. N., Hsu, J. H., Chen, Y. S. & Lin, J. G. Magnetoelectric response in lead-free multiferroic NiFe₂O₄-Na_{0.5}Bi_{0.5}TiO₃ composites. *J. Appl. Phys.* **109**, 07D904–3 (2011).
- Mukherjee, D. *et al.* Role of epitaxy in controlling the magnetic and magnetostrictive properties of cobalt ferrite-PZT bilayers. *J. Phys. D: Appl. Phys.* **43**, 485001–8 (2010).
- Cao, Y., Kobayashi, N., Zhang, Y. W., Ohnuma, S. & Masumoto, H. Enhancement of low-field magneto-dielectric response in two-dimensional Co/AlF granular films. *Appl. Phys. Lett.* **110**, 072902–5 (2017).
- Patil, D. R. *et al.* Significant enhancement of resonance magnetoelectric coupling in miniaturized lead-free NiFe₂O₄-BaTiO₃ multilayers. *Curr. Appl. Phys.* **17**, 1046–1049 (2017).
- Singh, G. M. K., Kumar, A., Dussan, S. & Katias, R. S. Multiferroics properties in BiFeO₃/CoFe₂O₄ heterostructures thin films deposited on (111)SrTiO₃. *AIP Conference Proceedings*, **1731**, 080043 (2016).
- Zhang, L., Zhai, J., Mo, W. & Yao, X. The dielectric and leakage current behavior of CoFe₂O₄-BaTiO₃ composite films prepared by combining method of sol-gel and electrophoretic deposition. *Solid State Sci.* **12**, 509–514 (2010).
- Spurgeon, S. R. *et al.* Thickness-Dependent Crossover from Charge- to Strain-Mediated Magnetoelectric Coupling in Ferromagnetic/Piezoelectric Oxide Heterostructures. *ACS NANO* **8**, 894–903 (2014).
- Kumari, M., Singh, A., Gupta, A., Prakash, C. & Chatterjee, R. Self-biased large magnetoelectric coupling in co-sintered Bi_{0.5}Na_{0.5}TiO₃ based piezoelectric and CoFe₂O₄ based magnetostrictive bilayered composite. *J. Appl. Phys.* **116**, 244101–5 (2014).
- Srinivas, A. *et al.* Observation of direct and indirect magnetoelectricity in lead free ferroelectric (Na_{0.5}Bi_{0.5}TiO₃)-magnetostrictive (CoFe₂O₄) particulate composite. *Appl. Phys. Lett.* **101**, 082902 (2012).
- Babu, S. N. & Malkinski, L. Observation of direct and indirect magnetoelectricity in lead free ferroelectric (Na_{0.5}Bi_{0.5}TiO₃)-magnetostrictive (CoFe₂O₄) particulate composite. *J. Appl. Phys.* **111**, 07D919 (2012).
- Babu, S. N., Min, S. G. & Malkinski, L. Electric field tunable magnetic properties of lead-free Na_{0.5}Bi_{0.5}TiO₃-CoFe₂O₄ multiferroic composites. *J. Appl. Phys.* **109**, 07D911 (2011).
- Zhou, J. P., Qiu, Z. C. & Liu, P. Electric and magnetic properties of Pb(Zr_{0.52}Ti_{0.48})O₃-CoFe₂O₄ particle composite thin film on the SrTiO₃ substrate. *Mater. Res. Bull.* **43**, 3514–3520 (2008).
- Park, J. S. *et al.* Enhanced Piezoelectric Properties of Lead-free 0.935(Bi_{0.5}Na_{0.5})TiO₃-0.065BaTiO₃ Thin Films Fabricated by Using Pulsed Laser Deposition. *J. Korean Phys. Soc.* **62**, 1031–1034 (2013).
- Takenaka, T., Maruyama, K. & Sakata, K. (Bi_{1/2}Na_{1/2})TiO₃-BaTiO₃ system for lead-free piezoelectric ceramics. *Jpn. J. Appl. Phys.* **30**, 2236–9 (1991).
- Li, H., Feng, C. & Yao, W. Some effects of different additives on dielectric and piezoelectric properties of (Bi_{1/2}Na_{1/2})TiO₃-BaTiO₃ morphotropic phase-boundary composition. *Mater. Lett.* **58**, 1194–1198 (2004).
- Chen, M. *et al.* Structure and electrical properties of (Na_{0.5}Bi_{0.5})_(1-x)Ba_xTiO₃ piezoelectric ceramics. *J. Eur. Ceram. Soc.* **28**, 843–849 (2008).
- Xu, Q. *et al.* Synthesis and piezoelectric and ferroelectric properties of (Na_{0.5}Bi_{0.5})_(1-x)Ba_xTiO₃ ceramics. *Mater. Chem. Phys.* **90**, 111–115 (2005).
- Dai, Y. Q. *et al.* Cation distribution in cobalt ferrite-aluminates. *J. Magn. Magn. Mater.* **394**, 287–291 (2015).
- Popescu, M. & Ghizdeanu, C. Cation Distribution in Cobalt Ferrite-Aluminates. *Phys. Status Solidi A* **52**, K169–K172 (1979).

28. Jones, G. O. & Thomas, P. A. The tetragonal phase of $\text{Na}_{0.5}\text{Bi}_{0.5}\text{TiO}_3$ - a new variant of the perovskite structure. *Acta Crystallogr. Sec. B: Struct. Sci.* **56**, 426–430 (2000).
29. Xu, C., Lin, D. & Kwok, K. W. Structure, electrical properties and depolarization temperature of $(\text{Bi}_{0.5}\text{Na}_{0.5})\text{TiO}_3$ - BaTiO_3 lead-free piezoelectric ceramics. *Solid State Sci.* **10**(10), 934–940 (2008).
30. Cernea, M., *et al* Electric and magnetic properties of ferromagnetic/piezoelectric bilayered composite. *J. Mater. Sci.* <https://doi.org/10.1007/s10853-018-2673-x>. (2018).
31. Walther, T. *et al*. BaTiO_3 - CoFe_2O_4 - BaTiO_3 trilayer composite thin films prepared by chemical solution deposition. *J. Eur. Ceram. Soc.* **36**, 559–565 (2016).
32. Tuan, N. H. *et al*. Structural, optical, and magnetic properties of lead-free ferroelectric $\text{Bi}_{0.5}\text{K}_{0.5}\text{TiO}_3$ solid solution with BiFeO_3 materials. *J. Electron. Mater.* **46**, 3472–3478 (2017).
33. Tolea, F., Grecu, M. N., Kuncser, V., Constantinescu, S. G. & Ghica, D. On the role of Fe ions on magnetic properties of doped TiO_2 nanoparticles. *Appl. Phys. Lett.* **106**(142404), 1–5 (2015).
34. Sundaresan, A., Bhargavi, R., Rangarajan, N., Siddesh, U. & Rao, C. N. R. Ferromagnetism as a universal feature of nanoparticles of the otherwise nonmagnetic oxides. *Phys Rev. B* **74**(161306), 1–4 (2006).
35. Wang, L. L., Wang, X. & Zheng, T. Structural and magnetic properties of nanocrystalline Fe-N thin films and their thermal stability. *J. Alloys Compd.* **443**, 43–47 (2007).
36. Kanamadi, C. M. *et al*. Magnetolectric and dielectric properties of $\text{Ni}_{0.5}\text{Cu}_{0.5}\text{Fe}_2\text{O}_4$ - $\text{Ba}_{0.5}\text{Pb}_{0.5}\text{Ti}_{0.5}\text{Zr}_{0.5}\text{O}_3$ ME composites. *J. Mater. Sci.* **42**, 5080–5084 (2007).
37. Testino, A. *et al*. Preparation of multiferroic composites of BaTiO_3 - $\text{Ni}_{0.5}\text{Zn}_{0.5}\text{Fe}_2\text{O}_4$ ceramics. *J. Eur. Ceram. Soc.* **26**, 3031–3036 (2006).
38. Chen, Q., Du, P. Y., Jin, L., Weng, W. J. & Han, G. R. Percolative conductor/polymer composite films with significant dielectric properties. *Appl. Phys. Lett.* **91**, 022912 (2007).
39. Zhou, Z. H., Xue, J. M., Li, W. Z. & Wang, J. Ferroelectric and electrical behavior of $(\text{Na}_{0.5}\text{Bi}_{0.5})\text{TiO}_3$ thin films. *J. Appl. Phys. Lett.* **85**, 804–806 (2004).
40. Pabst, G. W., Martin, L. W., Chu, Y. H. & Ramesh, R. Leakage mechanisms in BiFeO_3 thin films. *Appl. Phys. Lett.* **90**, 072902 (2007).
41. Sze, S. M. *Physics of Semiconductor Devices*. John Wiley & Sons, Hoboken, New Jersey, 2007.
42. Cernea, M. *et al*. CoFe_2O_4 magnetic ceramic derived from gel and sintered by spark plasma sintering. *J. Alloys Compd.* **656**, 854 (2016).
43. Cernea, M., Trupina, L., Dragoi, C., Galca, A. C. & Trinca, L. Structural, optical, and electric properties of BNT- $\text{BT}_{0.08}$ thin films processed by sol-gel technique. *J. Mater. Sci.* **47**, 6966–6971 (2012).
44. Sim, C. H., Pan, Z. Z. & Wang, J. Residual stress and magnetic behavior of multiferroic $\text{CoFe}_2\text{O}_4/\text{Pb}(\text{Zr}_{0.52}\text{Ti}_{0.48})\text{O}_3$ thin films. *J. Appl. Phys.* **105**, 084113 (2009).

Acknowledgements

The authors gratefully acknowledge the Romanian Government under POS-CCE project CEUREMAVSU Nr. 01/01.03.2009 allowing the acquisition of the research infrastructure. The SEM equipment was bought due to EU-funding grant POSCCE-A2-O2.2.1–2013–1/Priority direction 2, Project No. 638/12.03.2014, cod SMIS-CSNR 48652.

Author Contributions

M.C. designed the study and synthesized the samples. F.C. carried out dielectric spectroscopy, tunability and leakage current measurements and data analysis. B.S. Vasile performed TEM characterization. V.A.S. performed XRD measurements and carried out local piezoelectric and local magnetic properties measurements of the samples. R.T. performed SEM characterization. C.B. carried out magnetic property measurements and data analysis. M.C. and C.G. prepared the manuscript with contributions from all authors. All authors discussed the results and implications and participated to text revision.

Additional Information

Competing Interests: The authors declare no competing interests.

Publisher's note: Springer Nature remains neutral with regard to jurisdictional claims in published maps and institutional affiliations.



Open Access This article is licensed under a Creative Commons Attribution 4.0 International License, which permits use, sharing, adaptation, distribution and reproduction in any medium or format, as long as you give appropriate credit to the original author(s) and the source, provide a link to the Creative Commons license, and indicate if changes were made. The images or other third party material in this article are included in the article's Creative Commons license, unless indicated otherwise in a credit line to the material. If material is not included in the article's Creative Commons license and your intended use is not permitted by statutory regulation or exceeds the permitted use, you will need to obtain permission directly from the copyright holder. To view a copy of this license, visit <http://creativecommons.org/licenses/by/4.0/>.

© The Author(s) 2018